American Ecological Engineering Society

Journal of Ecological Engineering Design
journals.uvm.edu/jeed

Supplementary Material

Assessing Environmental Drivers of Denitrification in Restored Riverine Floodplains

Danielle Winter Lay[1], Sara W. McMillan[2], Jacob D. Hosen[3], Sayan Dey[4], Gregory B. Noe[5]

[1]Purdue Extension, Purdue University, West Lafayette, Indiana, United States
[2]Agricultural and Biosystems Engineering, Iowa State University, Ames, Iowa, United States
[3]Forestry and Natural Resources, Purdue University, West Lafayette, Indiana, United States
[4]Taylor Geospatial Institute, Saint Louis University, St. Louis, Missouri, United States
[5]U.S. Geological Survey, Florence Bascom Geoscience Center, Reston, Virginia, United States

Any use of trade, firm, or product names is for descriptive purposes only and does not imply endorsement by the U.S. Government.

Correspondence
Danielle Winter Lay
Purdue Extension
Purdue University
West Lafayette, IN 47907, USA
Email: winter35@purdue.edu

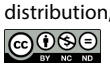

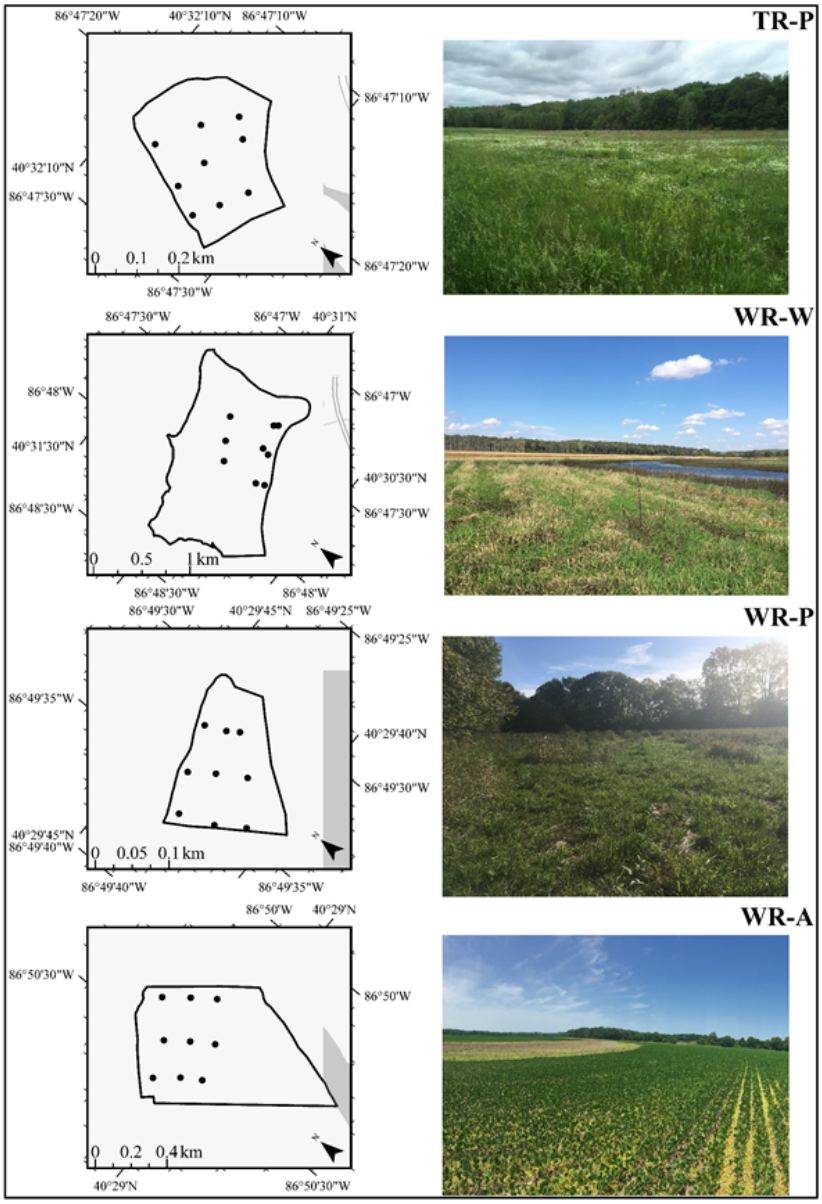

Figure S1 Detailed site maps and site photographs. Sampling locations within each site and photographs of each site, moving from upstream to downstream sites.

Table S1 Classification accuracy of remotely sensed vegetation data. Surface reflectance images were acquired from Landsat 8 and Sentinel-2 platforms. Surface reflectance compensates for the effects of different incoming solar radiation. For both platforms, images were only used if there was no cloud cover above the study sites and if the date on which the image was taken was close to the dates of field sampling. Imagery data were obtained from the U.S. Geological Survey (USGS) EarthExplorer over the confluence of the Wabash and Tippecanoe Rivers from the Operational Land Imager (OLI) sensor on the Landsat 8 platform. These images had a spatial resolution of 30 m for coastal aerosol, blue, green, red, near-infrared (NIR), and two short-wave infrared (SWIR) bands. Surface reflectance images were acquired on 3/19/2018, 6/7/2018, 8/26/2018, and 10/29/2018. Imagery data were acquired from the Copernicus Open Access Hub over the confluence of the Wabash and Tippecanoe Rivers from the Multispectral Instrument (MSI) onboard the Sentinel-2 platform. These images had a spatial resolution of 10 m (Spring 2019, Summer 2019, and Fall 2019) and 20 m (Winter 2019) for blue, green, red, and NIR bands. Surface reflectance products with Level 2A processing from Sentinel-2 were acquired for 12/19/2018, 4/1/2019, 6/30/2019, and 10/8/2019, which complement Winter 2019, Spring 2019, Summer 2019, and Fall 2019 sampling dates. Level-2A data from Sentinel-2 at these sites was unavailable prior to December 2018 in Copernicus Open Access Hub, which means that Summer 2018 and Fall 2018 do not have Sentinel-2 coverage. Landsat-8 data were used for sampling dates prior to December 2018, because Sentinel-2 data were not yet available. We performed supervised classification of vegetation and created feature space images for each seasonal image for every combination of bands with ERDAS Imagine (Hexagon AB, Stockholm, SE). Signatures were developed from combinations of bands that provided the greatest differentiation. We linked cursors between the feature space image and the satellite image and drew polygons in the feature space to encompass different vegetation types and other land use classes that were distinct in the feature space image. These polygons were used to calculate statistics for the spectral signatures of each vegetation or land use class, which were compiled in ERDAS's Signature Editor. One set of signatures was developed for each season. Based on these collections of signatures, each seasonal image was classified with the non-parametric method of feature space extraction. Pixels that overlapped or were outside of defined boundaries of signatures remained unclassified. Accuracy of classification was assessed with the Accuracy Assessment tool in ERDAS IMAGINE. We assessed the accuracy of classification by placing thirty points over the original raster image with stratified random sampling; assigning a class to each of these points based on our external reference information (i.e., ground-truthing, field notes, and site photographs); and comparing the user-defined class and class from supervised classification. We calculated overall classification accuracies and Kappa coefficients based on contrasting user-defined classes and supervised classification. Classifications from multiple images collected across seasons were used to select a single class for each sampling location to represent vegetation in a particular growing season. In certain seasons, vegetation types may be more readily discriminated, so the use of multiple seasons improves classification accuracy even further.

Imagery Source	Season	Overall Classification Accuracy	Overall Kappa
Sentinel-2	Winter 2019	50.0	0.43
Sentinel-2	Spring 2019	56.7	0.51
Sentinel-2	Summer 2019	76.7	0.71
Sentinel-2	Fall 2019	73.3	0.69
Sentinel-2	**2019 Growing Season**	85.2%	-
Landsat 8	Spring 2018	56.7	0.41
Landsat 8	Summer 2018	56.7	0.48
Landsat 8	Fall 2018 (Pre-Harvest)	26.7	0.18
Landsat 8	Fall 2018 (Post-Harvest)	43.3	0.37
Landsat 8	**2018 Growing Season**	77.8%	-

Table S2 Water chemistry of river water samples. Water chemistry of river water samples that were added to soils for ambient denitrification (DEA_{River}) measurements. We collected river water concurrently with soils each season from a channel adjacent to each floodplain site. The floodplain wetland site (WR-W) was at the confluence of the Tippecanoe River (TR) and the Wabash River (WR), but we collected water from the Tippecanoe River for DEA_{River} measurements for WR-W. Samples for the agricultural site (WR-A) and the prairie site on the mainstem of the Wabash River (WR-P) were collected from the Wabash River. Samples for the prairie site on the mainstem of the Tippecanoe River (TR-P) were also collected from the Tippecanoe River. We filtered samples through 0.45 µm nitrocellulose filters and froze the filtrate until analyses. We analyzed samples for concentrations of NO_3-N+NO_2-N (NO_3^-) (EPA-114-A Rev. 9), ortho-phosphate-P (PO_4^{3-}) (EPA-118 -A Rev. 5), and ammonium-N (EPA-103-A Rev. 10) with a SEAL AQ2 discrete analyzer (SEAL Analytical, Inc., Mequon, Wisconsin, US) and of non-purgeable dissolved organic carbon (DOC) concentrations on a TOC-$V_{CPH/CPN}$ Analyzer (Shimazdu Corporation, Kyoto, JP). ND indicates that a sample is below the limits of detection.

River	Sampling Date	Season	NO_3^- (mg N/L)	NH_4^+ (mg N/L)	PO_4^{3-} (mg P/L)	DOC (mg C/L)
WR-A	6/11/2018	Summer	4.74	0.062	0.019	9.1
WR-W	6/11/2018	Summer	4.55	0.108	0.015	8.8
TR-P	6/11/2018	Summer	6.28	0.130	0.028	8.7
WR-P	6/11/2018	Summer	4.33	0.078	0.005	8.9
WR-A	10/8/2018	Fall	2.73	0.042	0.021	9.0
WR-W	10/8/2018	Fall	1.55	0.051	0.052	9.9
TR-P	10/8/2018	Fall	2.70	0.037	0.040	9.6
WR-P	10/8/2018	Fall	2.05	0.009	0.038	11.1
WR-A	1/14/2019	Winter	5.81	0.112	0.027	6.0
WR-W	1/14/2019	Winter	6.37	ND	0.003	6.8
TR-P	1/14/2019	Winter	6.14	ND	0.011	5.3
WR-P	1/14/2019	Winter	5.20	ND	0.003	6.4
WR-A	4/4/2019	Spring	3.42	0.046	0.033	7.7
WR-W	4/4/2019	Spring	4.25	0.041	0.013	8.4
TR-P	4/4/2019	Spring	3.86	0.033	0.021	7.8
WR-P	4/4/2019	Spring	3.68	0.047	0.027	8.7
WR-A	7/15/2019	Summer	2.16	0.033	0.021	7.5
WR-W	7/15/2019	Summer	1.98	0.014	0.023	8.6
TR-P	7/15/2019	Summer	1.88	0.013	0.002	8.2
WR-P	7/15/2019	Summer	2.18	0.017	0.001	8.0
WR-A	10/21/2019	Fall	1.67	0.009	0.003	5.9
WR-W	10/21/2019	Fall	1.76	0.013	0.003	6.5
TR-P	10/21/2019	Fall	1.64	0.010	0.003	6.3
WR-P	10/21/2019	Fall	1.72	0.011	0.003	5.9
WR-A	1/27/2020	Winter	3.98	0.104	0.084	6.3
WR-W	1/27/2020	Winter	4.65	0.074	0.007	5.8
TR-P	1/27/2020	Winter	4.94	0.060	0.024	6.5
WR-P	1/27/2020	Winter	4.17	0.093	0.081	4.9
WR-A	5/7/2020	Spring	3.35	0.024	0.006	4.2
WR-W	5/7/2020	Spring	4.09	0.015	0.012	5.0
TR-P	4/20/2020	Spring	2.75	0.018	0.003	5.4
WR-P	5/7/2020	Spring	4.22	0.013	0.003	4.1

Table S3 Cumulative days of inundation. We estimated the cumulative days inundated for each of the 36 sampling locations across the four sites [WR-A: row crop agriculture along the Wabash River; WR-W: mitigation wetland restoration project at a former agriculture site along the Wabash River; TR-P: former agriculture site along the Tippecanoe River that was restored as a prairie; WR-P: former agriculture site along the Wabash River that was restored as a prairie] based on the HEC-RAS time series of inundation depths. Days of inundation were summed across each calendar year.

Site	Sampling Location	2018 (days)	2019 (days)	2020 (days)
WR-A	1	57	50	22
WR-A	2	17	2	1
WR-A	3	16	2	1
WR-A	4	37	19	9
WR-A	5	124	151	77
WR-A	6	10	0	0
WR-A	7	56	48	21
WR-A	8	90	100	48
WR-A	9	27	8	5
WR-A	**Mean**	**48.2**	**42.2**	**20.4**
WR-W	1	40	21	10
WR-W	2	58	47	21
WR-W	3	83	91	43
WR-W	4	53	39	18
WR-W	5	87	99	47
WR-W	6	232	343	156
WR-W	7	56	43	19
WR-W	8	304	447	207
WR-W	9	42	24	12
WR-W	**Mean**	**106.1**	**128.2**	**59.2**
TR-P	1	0	0	0
TR-P	2	8	0	0
TR-P	3	67	53	24
TR-P	4	3	0	0
TR-P	5	19	1	1
TR-P	6	51	28	13
TR-P	7	14	1	0
TR-P	8	64	60	25
TR-P	9	21	2	1
TR-P	**Mean**	**27.4**	**16.1**	**7.1**
WR-P	1	39	23	10
WR-P	2	18	2	1
WR-P	3	28	8	5
WR-P	4	31	13	6
WR-P	5	19	3	2
WR-P	6	12	1	0
WR-P	7	31	13	7
WR-P	8	20	3	2
WR-P	**Mean**	**23.7**	**7.4**	**3.8**

Table S4. *Post hoc* pairwise testing by site. Summary of output from pairwise Tukey contrasts of denitrification metrics across sites [WR-A: row crop agriculture along the Wabash River; WR-W: mitigation wetland restoration project at a former agriculture site along the Wabash River; TR-P: former agriculture site along the Tippecanoe River that was restored as a prairie; WR-P: former agriculture site along the Wabash River that was restored as a prairie]. Ambient (DEA_{River}) and potential (DEA_{CN}) denitrification were square-root-transformed, and estimates of pairwise differences (ΔDEA) are reported as log-transformed values. Bolded p-values are significant.

Measure	Group 1	Group 2	Estimate of Difference [Group 1-Group 2]	Lower Bound of 95% Confidence Interval of Difference	Upper Bound of 95% Confidence Interval of Difference	p-value
DEA_{River}	WR-A	WR-W	-0.521	-0.649	-0.394	**<0.001**
DEA_{River}	WR-A	TR-P	-0.314	-0.441	-0.186	**<0.001**
DEA_{River}	WR-A	WR-P	-0.435	-0.563	-0.307	**<0.001**
DEA_{River}	WR-W	TR-P	0.207	0.080	0.335	**0.001**
DEA_{River}	WR-W	WR-P	0.086	-0.041	0.214	0.277
DEA_{River}	TR-P	WR-P	-0.121	-0.249	0.006	0.067
DEA_{CN}	WR-A	WR-W	-0.470	-0.647	-0.293	**<0.001**
DEA_{CN}	WR-A	TR-P	-0.265	-0.442	-0.087	**0.002**
DEA_{CN}	WR-A	WR-P	-0.559	-0.736	-0.382	**<0.001**
DEA_{CN}	WR-W	TR-P	0.205	0.028	0.382	**0.018**
DEA_{CN}	WR-W	WR-P	-0.089	-0.266	0.088	0.533
DEA_{CN}	TR-P	WR-P	-0.294	-0.471	-0.117	**<0.001**
ΔDEA	WR-A	WR-W	-0.521	-0.649	-0.394	**<0.001**
ΔDEA	WR-A	TR-P	-0.314	-0.441	-0.186	**<0.001**
ΔDEA	WR-A	WR-P	-0.435	-0.563	-0.307	**<0.001**
ΔDEA	WR-W	TR-P	0.207	0.080	0.335	**0.001**
ΔDEA	WR-W	WR-P	0.086	-0.041	0.214	0.277
ΔDEA	TR-P	WR-P	-0.121	-0.249	0.006	0.067

Table S5. *Post hoc* pairwise testing by season. Summary of outputs from pairwise Tukey contrasts of denitrification metrics across seasons. Ambient (DEA_{River}) and potential (DEA_{CN}) denitrification were square-root-transformed, and ΔDEA was log-transformed with an offset. Estimates of pairwise differences are reported as transformed values. Bolded p-values are significant.

Measure	Group 1	Group 2	Estimate of Difference [Group 1-Group 2]	Lower Bound of 95% Confidence Interval of Difference	Upper Bound of 95% Confidence Interval of Difference	p-value
DEA_{River}	Fall	Spring	-0.013	-0.079	0.054	0.963
DEA_{River}	Fall	Summer	0.053	-0.015	0.121	0.186
DEA_{River}	Fall	Winter	-0.079	-0.146	-0.012	**0.013**
DEA_{River}	Spring	Summer	0.065	-0.003	0.133	0.064
DEA_{River}	Spring	Winter	-0.067	-0.133	0.000	0.052
DEA_{River}	Summer	Winter	-0.132	-0.200	-0.064	**<0.001**
DEA_{CN}	Fall	Spring	-0.051	-0.130	0.027	0.332
DEA_{CN}	Fall	Summer	-0.188	-0.284	-0.091	**<0.001**
DEA_{CN}	Fall	Winter	-0.105	-0.184	-0.026	**0.004**
DEA_{CN}	Spring	Summer	-0.136	-0.233	-0.040	**0.002**
DEA_{CN}	Spring	Winter	-0.054	-0.133	0.025	0.295
DEA_{CN}	Summer	Winter	0.082	-0.015	0.179	0.126
ΔDEA	Fall	Spring	-0.030	-0.083	0.024	0.480
ΔDEA	Fall	Summer	-0.090	-0.156	-0.024	**0.003**
ΔDEA	Fall	Winter	-0.017	-0.071	0.037	0.849
ΔDEA	Spring	Summer	-0.060	-0.125	0.005	0.082
ΔDEA	Spring	Winter	0.013	-0.041	0.066	0.924
ΔDEA	Summer	Winter	0.073	0.008	0.138	**0.022**

Table S6. Mean and standard error of ambient (DEA_{River}) and potential (DEA_{CN}) denitrification by restoration design approach. Summary statistics for prairie include prairies along the Tippecanoe River (TR-P) and Wabash River (WR-P). (DEA_{River} number of observations (n): Agriculture (WR-A) =70, Prairie (P) =142, Wetland (WR-W) =63; DEA_{CN} (n): Agriculture=62, Prairie=126, Wetland=63).

Measure	Agriculture (WR-A)	Prairie (WR-P & TR-P)	Wetland (WR-W)
DEA_{River} (μg N_2O-N/hour/g dry soil)	0.183±0.014	0.634±0.024	0.887±0.047
DEA_{CN} (μg N_2O-N/hour/g dry soil)	0.330±0.023	0.961±0.047	1.077±0.089

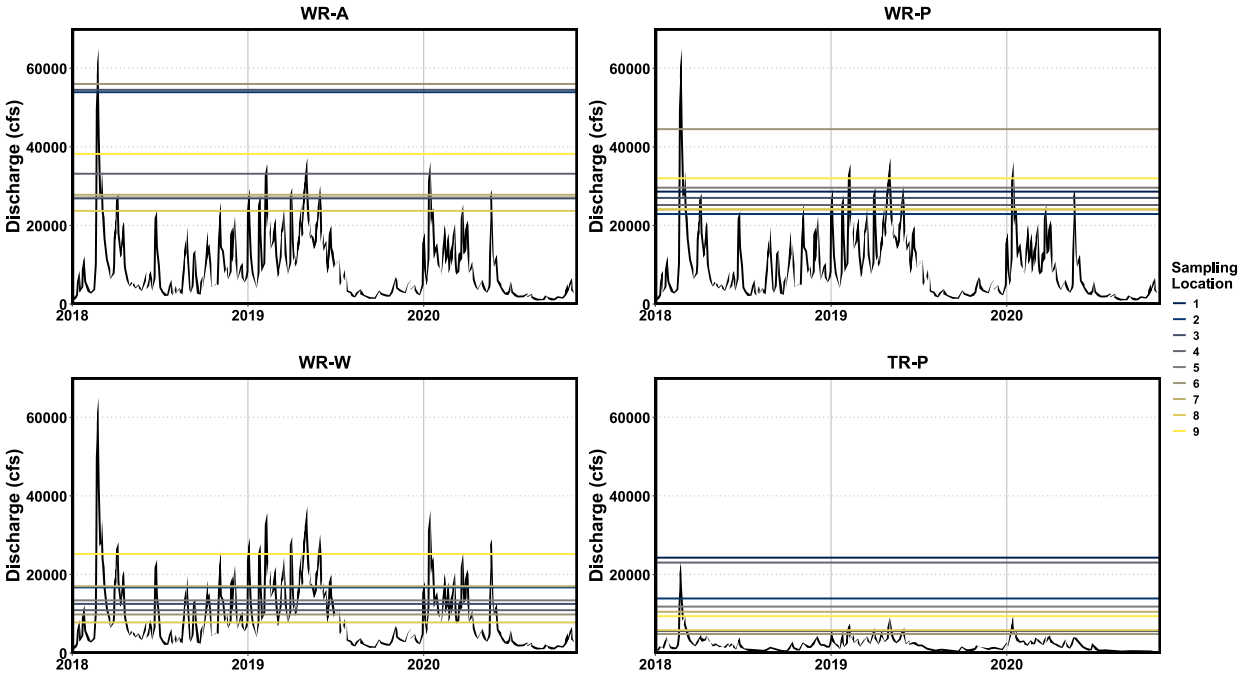

Figure S2. Time series of river discharge and indicators of inundation discharge. Mean daily discharge for the gages downstream of WR-A (row crop agriculture along the Wabash River), WR-P (former agriculture site along the Wabash River that was restored as a prairie), and WR-W (mitigation wetland restoration project at a former agriculture site along the Wabash River) (USGS 03335500) and upstream of TR-P (former agriculture site along the Tippecanoe River that was restored as a prairie) (USGS 03332605) (U.S. Geological Survey 2021). Horizontal lines represent discharge at which inundation is likely to occur due to overbank flooding for each sampling location.

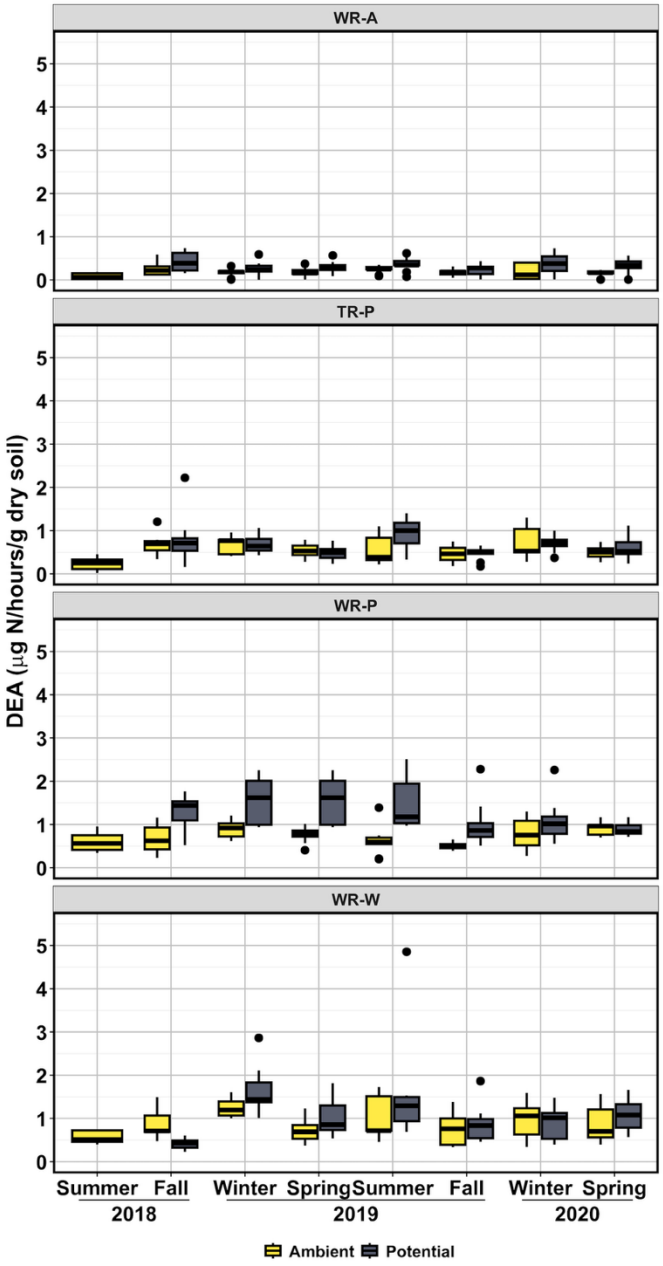

Figure S3. Boxplots of denitrification enzyme activity parsed by the season and year. The horizontal black bar represents the median denitrification. Edges of the box represent the interquartile range. Whiskers represent the threshold for outliers based on the interquartile criteria. Black points are outliers. [WR-A: row crop agriculture along the Wabash River; WR-W: mitigation wetland restoration project at a former agriculture site along the Wabash River; TR-P: former agriculture site along the Tippecanoe River that was restored as a prairie; WR-P: former agriculture site along the Wabash River that was restored as a prairie]

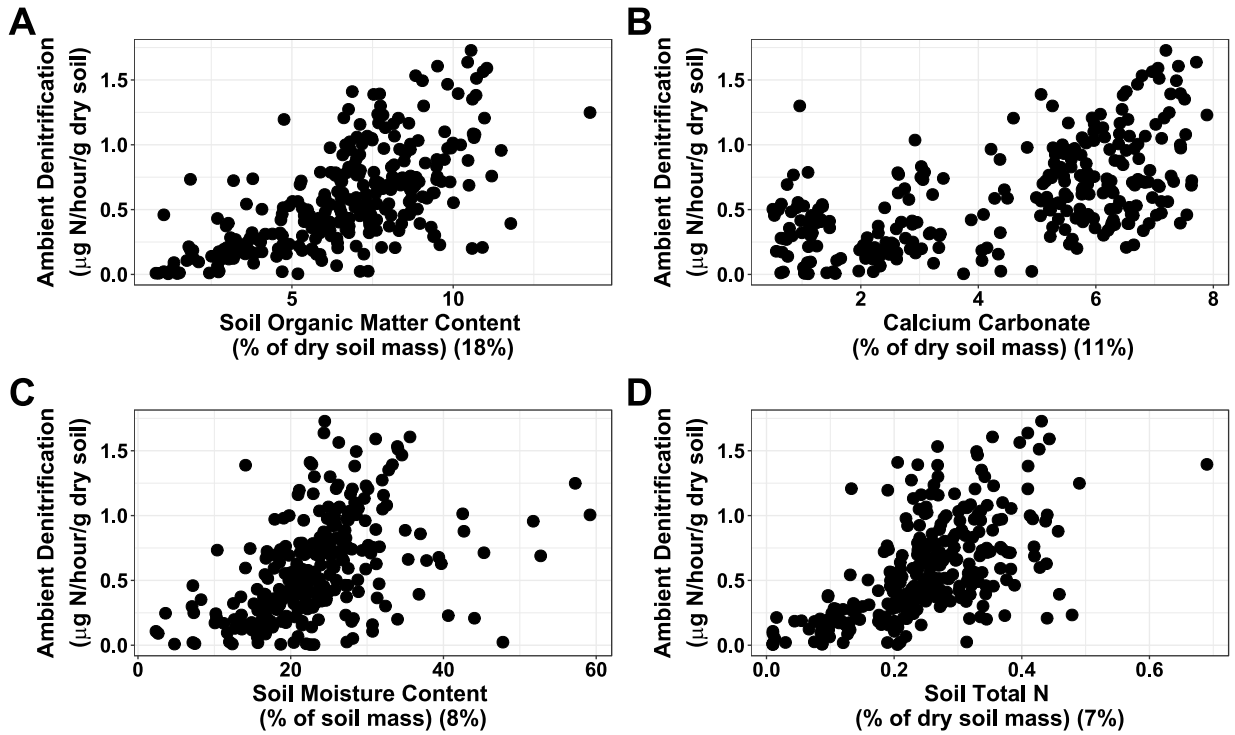

Figure S4. Bivariate relationships between ambient denitrification rates (DEA_{River}) and quantitative soil variables that were included in the boosted regression tree model of DEA_{River}. These soil variables are positively related to denitrification capacity.

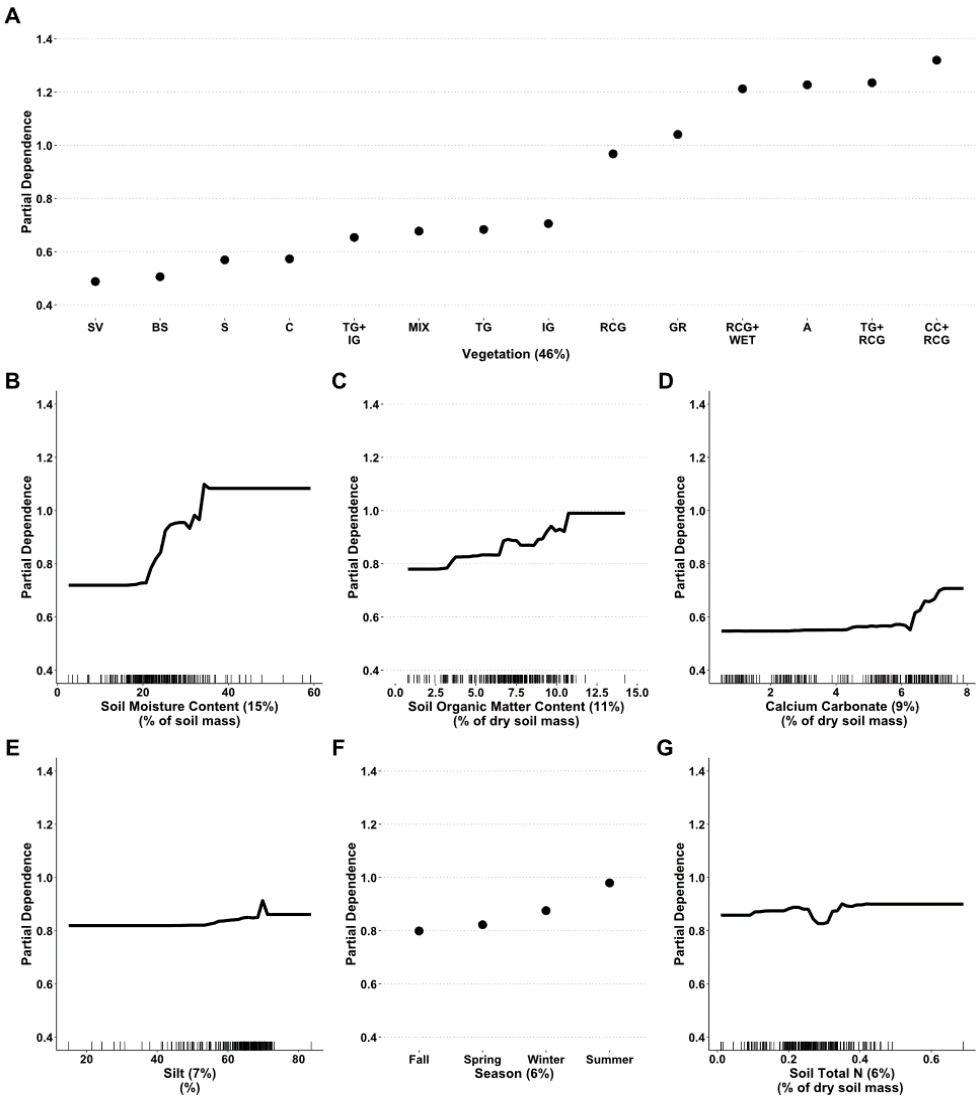

Figure S5. Partial dependence plot of the boosted regression tree model of potential denitrification (DEA_{CN}) A.) Plant communities* that were present in WR-A also supported low DEA_{CN}, but the ranking of plant communities that supported elevated DEA_{CN} differed slightly from those that supported high ambient denitrification (DEA_{River}); B.) Like DEA_{River}, DEA_{CN} rates were maximized when the soil moisture content was between 20% and 40%; C.) DEA_{CN} was positively associated with soil organic matter over a narrower range of 8% to 10%; D.) DEA_{River} and DEA_{CN} had similar relationships with calcium carbonate content; E.) DEA_{CN} was elevated during the summer and winter; F.) Denitrification was positively associated with soil total nitrogen but had a limited relationship beyond 0.4% soil total nitrogen; G.) Silt content was positively associated with denitrification. *[SV=sparsely vegetated, BS=bare soil, S=Soy, C=Corn, TG+IG=Tall Goldenrod and Indian Grass, MIX=mixed shrubs and grasses, TG=Tall Goldenrod, IG=Indian Grass, RCG=Reed Canary Grass, GR=Giant Ragweed, RCG+WET=Reed Canary Grass and obligate wetland plants, A=Amaranth, TG+RCG=Tall Goldenrod and Reed Canary Grass, CC+RCG=Cutleaf Coneflower and Reed Canary Grass]

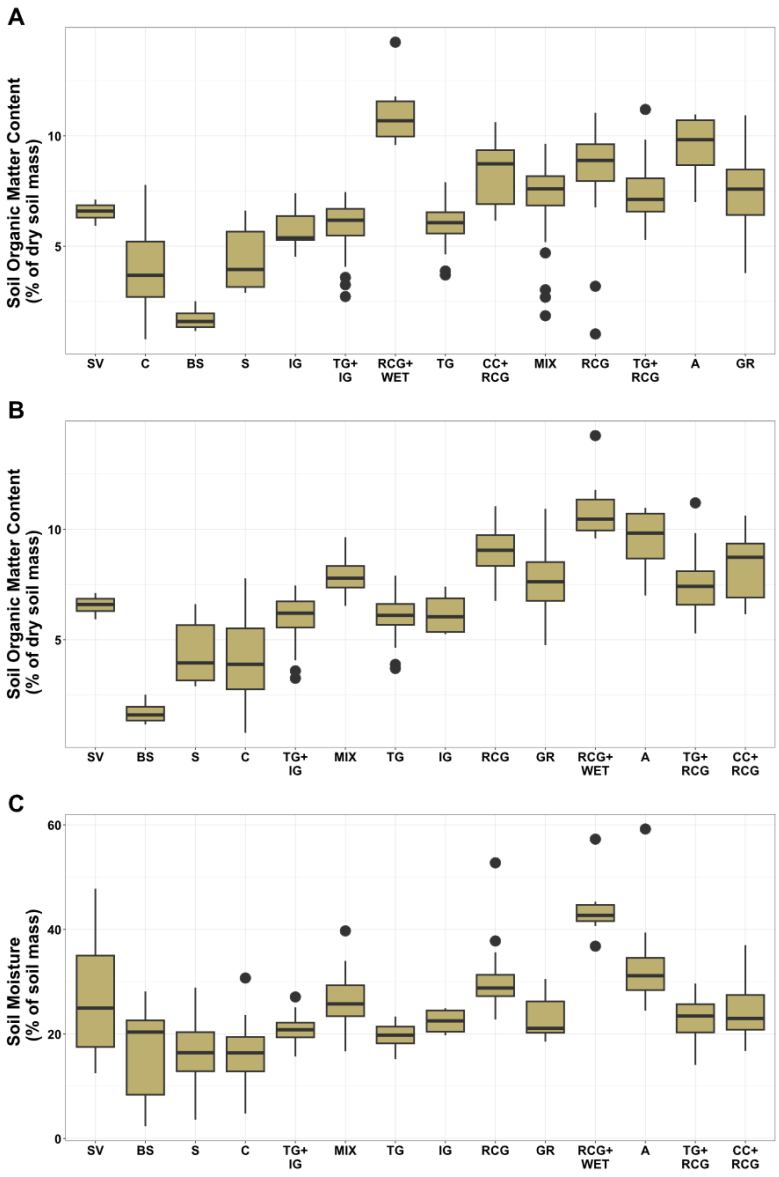

Figure S6. Boxplots to explore interactions between vegetation and soil properties in the boosted regression tree models. The black bar, edges of the box, and vertical lines represent medians, interquartile range, and threshold for outliers based on the interquartile range criteria, respectively. A.) Vegetation* interacted with soil organic matter in the ambient denitrification (DEA_{River}) boosted regression tree (BRT) model. Vegetation is ordered along the x-axis based on the partial dependence of DEA_{River} from least to greatest. Vegetation with the highest partial dependence of DEA_{River} also tended to have the highest soil organic matter; B.) Vegetation* is ordered along the x-axis based on partial dependence of potential denitrification (DEA_{CN}) from least to greatest to explore the interaction of soil organic matter and DEA_{CN} in the DEA_{CN} BRT model. Vegetation with higher partial dependence was associated with greater soil organic matter; C.) Soil moisture content and vegetation* interacted in the DEA_{CN} BRT model. Vegetation is ordered along the x-axis based on partial dependence of DEA_{CN} from least to greatest. Higher soil moisture is generally associated with vegetation types with higher DEA_{CN}. *[SV=sparsely vegetated, BS=bare soil, S=soy, C=corn, TG+IG=tall goldenrod and Indiangrass, MIX=mixed shrubs and grasses, TG=tall goldenrod, IG=Indiangrass, RCG=reed canary grass, GR=giant ragweed, RCG+WET=reed canary grass and a mix of obligate wetland plants, A=amaranth, TG+RCG=tall goldenrod and reed canary grass, CC+RCG=cutleaf coneflower and reed canary grass]

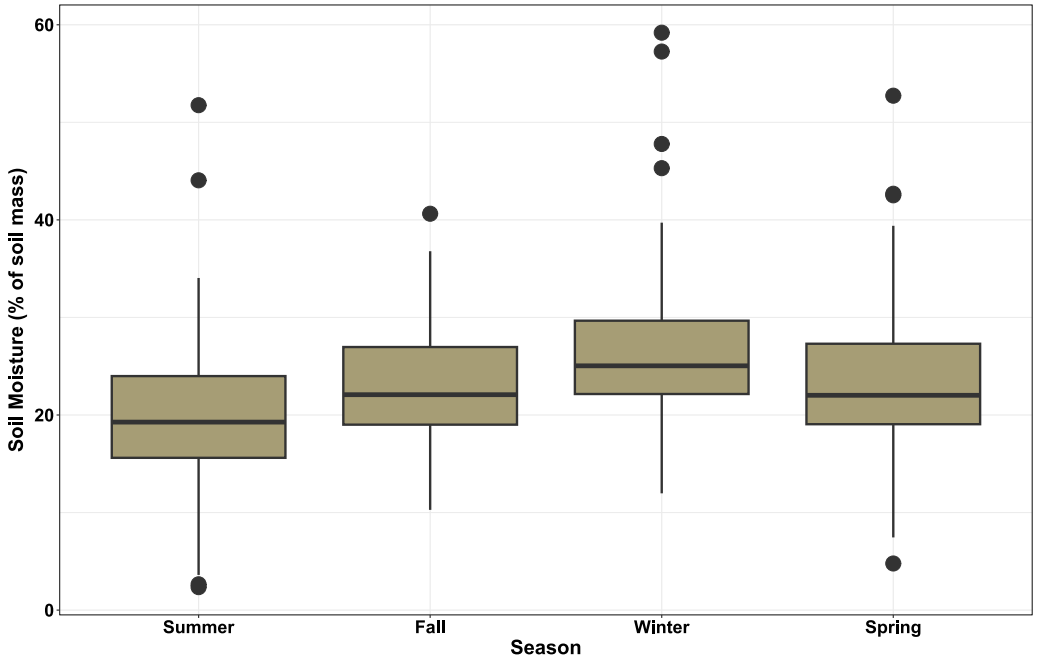

Figure S7. Boxplots of soil moisture content across seasons using median and interquartile range. Soil moisture content and season interacted in the ambient denitrification (DEA_{River}) boosted regression tree (BRT) model, such that seasons with higher DEA_{River} tended to have higher soil moisture.

Table S7. Correlation tests of denitrification rates with soil properties. Spearman's ρ gives the strength of association. The p-values above 0.05 indicate the correlation is not statistically significant. Bivariate relationships between denitrification rates and environmental properties potential (DEA_{CN}) and ambient (DEA_{River}) denitrification were significantly correlated with many of the same soil properties, and the correlation coefficients (ρ) for each variable were of similar magnitude. Samples from the prairie site along the Tippecanoe River (TR-P) and agricultural site along the Wabash River (WR-A) were often clustered in scatterplots with soil properties, while the floodplain wetland site (WR-W) and prairie site along the Wabash River (WR-P) were also grouped. Clay content, 10th percentile particle size, and 50th percentile particle size could not be linearized with the tested transformations, so we could not reliably test correlation. Bolded p-values are significant. *Correlation test is unreliable due to some deviations from linear associations.

	DEA_{River}		DEA_{CN}	
	ρ	**p-value**	**ρ**	**p-value**
Soil moisture content	0.600	0.051	0.591	0.056
Soil organic matter (SOM) content	0.827	**0.002**	0.882	**<0.001**
Soil total carbon (C) content	0.900	**<0.001**	0.845	**0.001**
Soil total nitrogen (N) content	0.882	**<0.001**	0.827	**0.002**
Soil carbon-to-nitrogen ratio (C:N)*	-0.318	0.340	-0.409	0.212
90th percentile particle size	-0.518	0.102	-0.518	0.102
Sand content*	-0.545	0.083	-0.545	0.083
Silt content	0.582	0.060	0.573	0.066
Calcium carbonate ($CaCO_3$) content	0.800	**0.003**	-0.800	**0.003**
Bulk density	-0.800	**0.003**	-0.781	**0.004**

Table S8. Mean and standard error of soil properties by site across seasons. *Bulk density was not measured for each sampling event, so the standard error is adjusted accordingly. [WR-A: row crop agriculture along the Wabash River; WR-W: mitigation wetland restoration project at a former agriculture site along the Wabash River; TR-P: former agriculture site along the Tippecanoe River that was restored as a prairie; WR-P: former agriculture site along the Wabash River that was restored as a prairie]

	WR-A	**TR-P**	**WR-P**	**WR-W**
Soil moisture content (%)	17.0±0.9	23.3±0.6	25.9±1.0	26.2±0.9
Soil organic matter (SOM) content (%)	3.9±0.2	6.9±0.2	8.0±0.20	7.8±0.3
Soil total carbon (C) content (%)	2.09±0.11	3.56±0.13	4.50±0.09	5.13±0.10
Soil total nitrogen (N) content (%)	0.13±0.01	0.27±0.01	0.28±0.01	0.31±0.01
Soil carbon-to-nitrogen ratio (C:N)	21.6±2.0	13.3±0.2	16.2±0.1	17.0±0.4
10^{th} percentile particle size (µm)	2.7±0.2	2.8±0.2	2.1±0.1	2.1±0.1
50^{th} percentile particle size (µm)	54.1±9.2	20.6±1.5	13.9±0.4	14.4±0.4
90^{th} percentile particle size (µm)	242.0±16.5	221.7±14.6	132.6±4.4	120.4±3.9
Sand content (%)	37.7±2.3	28.7±1.3	23.0±0.6	22.7±0.6
Silt content (%)	52.3±1.7	62.6±0.9	66.8±0.4	67.4±0.4
Clay content (%)	10.0±0.7	8.7±0.5	10.2±0.3	9.8±0.3
Calcium carbonate ($CaCO_3$) content (%)	2.5±0.1	2.3±0.2	5.7±0.1	6.8±0.1
Bulk density*	1.56±0.03	1.38±0.33	1.23±0.29	1.20±0.28

Table S9. Correlation tests of hydrogeomorphic properties with denitrification rates. Spearman's ρ gives the strength of association of hydrogeomorphic soil properties with potential (DEA_{CN}) and ambient (DEA_{River}) denitrification. The p-values above 0.05 indicate the correlation is not statistically significant. Among select hydrogeomorphic metrics, we only found a significant correlation of DEA_{River} with 10^{th} percentile flood velocity (ρ=0.742) and median flood velocity (ρ=0.660). No significant correlations were found between DEA_{CN} and the selected hydrogeomorphic metrics. Bolded p-values are significant. *Correlation test is unreliable due to some deviations from linear associations.

	DEA_{River}		**DEA_{CN}**	
	ρ	**p-value**	**ρ**	**p-value**
Horizontal distance to nearest drainage (HDND)	-0.222	0.309	0.018	0.960
Height above nearest drainage (HAND)*	-0.052	0.814	0.333	0.347
Slope to the nearest drainage	0.387	0.068	0.697	0.025
10^{th} percentile flood velocity	0.742	**<0.001**	0.358	0.310
Median flood velocity	0.660	**<0.001**	0.285	0.425
Maximum flood velocity	0.208	0.341	-0.212	0.556
Inundation in the past 30 days	0.143	0.516	-0.285	0.425
Inundation in the past 90 days	0.154	0.484	-0.139	0.701
Inundation in the past 180 days	0.111	0.613	-0.248	0.489

Table S10. Mean and standard error of hydrogeomorphic properties by site across seasons. [WR-A: row crop agriculture along the Wabash River; WR-W: mitigation wetland restoration project at a former agriculture site along the Wabash River; TR-P: former agriculture site along the Tippecanoe River that was restored as a prairie; WR-P: former agriculture site along the Wabash River that was restored as a prairie]

	WR-A	**TR-P**	**WR-P**	**WR-W**
Horizontal distance to nearest drainage (HDND) (ft)	1390±116	2577±150	2119±159	1826±188
Height above nearest drainage (HAND) (ft)	7.4±1.0	7.8±0.4	15.9±0.7	4.1±0.2
Slope to the nearest drainage (ft/ft)	0.006±0.001	0.005±0.001	0.011±0.001	0.010±0.001
10^{th} percentile flood velocity (ft/s)	0.01±0.001	<0.01±<0.001	0.01±0.002	0.02±0.002
Median flood velocity (ft/s)	0.08±0.01	0.02±<0.01	0.08±0.11	0.23±0.10
Maximum flood velocity (ft/s)	2.74±0.17	1.17±0.16	1.41±0.07	3.96±0.13
Inundation in the past 30 days (days)	2.7±0.7	0.9±0.3	0.6±0.2	3.2±0.6
Inundation in the past 90 days (days)	9.8±2.1	2.7±0.7	1.9±0.4	12.3±1.8
Inundation in the past 180 days (days)	19.3±3.5	5.9±1.2	4.8±0.7	24.9±3.0

References

U.S. Geological Survey. 2021. USGS water data for the Nation: U.S. Geological Survey National Water Information System database. https://doi.org/10.5066/F7P55KJN